*Y. Sun and M. Gupta**

Department of Mechanical Engineering-Engineering Mechanics, Michigan Technological University, Houghton, MI, USA

Effect of Elongational Viscosity on the Flow in a Flat Die

The flow of a low-density polyethylene in a flat die is simulated using the axisymmetric and planar elongational viscosities estimated in an earlier publication by Beaupre and Gupta. Elongational viscosity is found to have only a limited effect on the velocity distribution at the die exit. However, the predicted pressure drop in the die and the temperature distribution at the die exit changed significantly when the effect of elongational viscosity was included in the simulation.

1 Introduction

Screw extruders [1] are used to manufacture plastic parts for a large number of end-use applications such as pipes, sidings for building, seals for car windows, etc. Even though the same extruder can be used to manufacture many of these plastic parts, a different die is required for each product. The die determines the dimensions and quality of the extruded products. Therefore, use of an optimally designed die is crucial for the quality of the extruded parts. The main task in design of an extrusion die is to optimize the die channel geometry such that uniform velocity and temperature distributions are obtained at the die exit, without excessively increasing the pressure drop in the die [2]. This requires, an analysis of the velocity, pressure and temperature fields in the polymeric flow in the die. However, at present, most die designs for polymer extrusion are based upon the past experience of the designer, trial and error, or at most a flow simulation using the generalized Newtonian formulation [3 to 6]. A generalized Newtonian constitutive equation can accurately capture the strain-rate dependence of the shear viscosity of a polymer. However, the elongational viscosity predicted by the generalized Newtonian formulation is generally much smaller than the actual elongational viscosity of a polymer. Therefore, in applications involving elongation-dominated flows, such as extrusion dies, the velocity, pressure and temperature fields predicted by the generalized Newtonian formulation can have large errors. Even though some of the viscoelastic constitutive equations [7] can predict the high elongational viscosity of polymers, difficulty in convergence of viscoelastic flow simulations, along with the large computation time required for the simulation, and difficulty in finding the values of various parameters in the constitutive equations have limited the application of viscoelastic flow simulation in design of extrusion dies.

In the present work, the PELDOM software [8] was used for a three-dimensional simulation of the flow in a flat extrusion die. The software simulates a nonisothermal polymeric flow taking into account the strain-rate dependence of the shear as well as elongational viscosity of the polymer. The software has been shown to accurately capture the entrance pressure loss and recirculating vortices in a channel with an abrupt contraction [9 to 12]. The software is easy to use because instead of the various parameters, such as relaxation times, required for a typical viscoelastic simulation, for a three-dimensional simulation of a polymeric flow, the software requires a knowledge of the axisymmetric and planar elongational viscosities of the polymer. However, measurement of elongational viscosity of a polymer at high strain rates (100 to 10,000 s^{-1}), typically encountered in extrusion dies, is difficult. Most of the experimental techniques for direct measurement of elongational viscosity only measure the elongational viscosity at strain rates below 10 s^{-1} [13, 14]. The method used in the present work for estimating the elongational viscosity of a polymer is discussed next.

2 Elongational Viscosity Estimation

In the present work, the axisymmetric and planar elongational viscosities of a low-density polyethylene (Dow 132i) estimated by *Beaupre* and *Gupta* [15] were used to investigate the effect of elongational viscosity on the flow in a flat die. *Beaupre* and *Gupta* [15] used the entrance-flow method to estimate the axisymmetric and planar elongational viscosities of Dow 132i. In the entrance-flow method, the large pressure drop (entrance loss) encountered near an abrupt contraction in a channel (entrance flow), which increases as the elongational viscosity of the fluid is increased, and also depends on the flow rate in the channel, is used for an indirect measurement of the strain-rate dependence of the elongational viscosity of a polymer. In particular, *Beaupre* and *Gupta* [15] optimized the value of the four elongational viscosity parameters (δ, λ_1,λ_2, m) in the Sarkar-Gupta elongational viscosity model [16] (Eq. 1) such that the difference between the experimental value of the entrance pressure loss from a capillary or slit rheometer and the corresponding predictions from a finite-ele-

* Mail address: M. Gupta, Dept. of Mechanical Engineering-Engineering Mechanics, Michigan Technological University, 815 R. L. Smith-ME-EM Bldg., 1400 Townsend Drive, Houghton, MI49931-1295, USA

ment simulation is minimized.

$$\eta_e = \eta_0 \left[T_r + \delta \left\{ 1 - \frac{1}{\sqrt{1 + (\lambda_1 e_{II})^2}} \right\} \right] (1 + (\lambda_2 e_{II})^2)^{\frac{m-1}{2}} \quad (1)$$

where $e_{II} = \sqrt{2(\tilde{e} : \tilde{e})}$ is the second invariant of the strain-rate tensor $\tilde{e} = (\nabla\hat{v} + \nabla\hat{v}^T)/2$, with $\hat{v}$ being the velocity of the fluid, T_r, the Trouton ratio at low shear rate, is 3 for an axisymmetric flow and 4 for a planar flow, and $\eta_0, \delta, \lambda_1, \lambda_2$ and m are material parameters. To capture the strain-rate dependence of the shear viscosity of a polymer, the Carreau model [17] is used in this work:

$$\eta_s = \eta_0 (1 + (\lambda e_{II})^2)^{\frac{n-1}{2}} \quad (2)$$

where η_0, the zero-shear viscosity, is the same as in Eq. 1, and λ and n are the two new material parameters. The Arrhenius model [17] is used in this work to capture the temperature dependence of η_0 in Eqs. 1 and 2:

$$\eta_0 = A \exp\left(\frac{T_a}{T}\right) \quad (3)$$

where A and T_a are material parameters, and T is the temperature of the polymer.

For Dow 132i, *Beaupre* and *Gupta* [15] gave the Carreau model parameters for shear viscosity at 215 and 230 °C. The values of the Carreau model parameters given by *Beaupre* and *Gupta* [15] were used in the present work to obtain the parameters for the Carreau-Arrhenius model for Dow 132i:

$A = 469.0\ Pa \cdot s,\ T_a = 2721.7\ K,\ \lambda = 0.6509\ s,\ n = 0.401.$

By using the entrance-flow method for elongational viscosity estimation, for Dow 132i at 215 and 230 °C, *Beaupre* and *Gupta* [15] also gave the values of elongational viscosity parameters for the Sarkar-Gupta model. These values from reference [15] were used in the present work to obtain the temperature dependence of the Sarkar-Gupta model for axisymmetric and planar elongational viscosities.

Axisymmetric: $\delta = 0,\ \lambda_2 = 0.02242\ s,\ m = 0.349.$

Planar: $\delta = 37.3,\ \lambda_1 = 11.795\ s,\ \lambda_2 = 0.4571\ s,\ m = 0.45.$

It should be noted that λ in the Carreau model for shear viscosity, and λ_1 and λ_2 in the Sarkar-Gupta model for elongational viscosity depend upon temperature. Temperature dependence of λ, λ_1 and λ_2 can be easily obtained by using the time-temperature superposition principle [17] along with the Arrhenius model (Eq. 3).

Based upon the values of the parameters for the Carreau model and the Sarkar-Gupta model given above, the shear and elongational viscosities of Dow 132i at 215 and 230 °C are shown in Fig. 1. Fig. 1 also shows the elongational viscosity predicted by the Cogswell's [18] and Binding's [19] analyses. In general, the elongational viscosity estimated by Cogswell's and Binding's analyses are higher than the corresponding estimations by optimizing the values of elongational viscosity parameters in the Sarkar-Gupta model. The discrepancy is particularly large for the planar elongational viscosity. The predictions from Cogswell's analysis in Fig. 1 show that the average elongation rate for the experimental data on planar entrance loss is in the transition region between elongation thickening and elongation thinning portions of the elongational viscosity curve, which might have resulted in the large difference between the predictions from the Cogswell's and Binding's analyses and those from the finite-element simulation by *Beaupre* and *Gupta* [15]. Since the experimental data for the axisymmetric entrance flow is in the power-law region of the elongational viscosity, the predictions of *Beaupre* and *Gupta* are in better agreement with those from the Cogswell's and Binding's analyses.

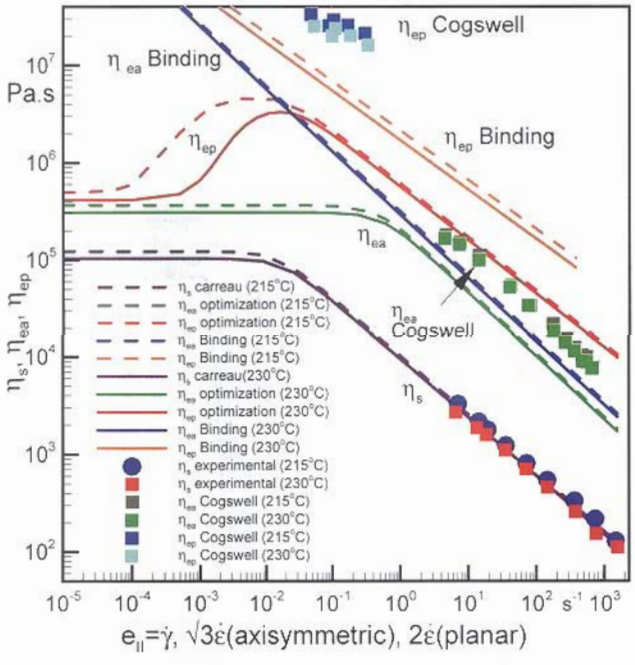

Fig. 1. Variation of shear (η_s) and elongational (η_{ep}(planar), η_{ea}(axisymmetric)) viscosities of LDPE with the second invariant of strain-rate tensor (e_{II})

3 Effect of Elongational Viscosity on the Flow in a Flat Die

In this section, the shear viscosity and the axisymmetric and planar elongational viscosities for Dow 132i, given in the last section, are used for a three-dimensional simulation of the flow in a flat extrusion die. Fig. 2 shows the geometry and the finite element mesh for the flat die used in this work. The tetrahedral finite elements employed in this work, use a linear interpolation for pressure and temperature, whereas a linear interpolation enriched with a piecewise-linear bubble function is used for the velocity interpolation over the tetrahedral finite elements [20]. However, the velocity equations corresponding to the bubble nodes are eliminated at the element level using the static condensation technique [21], resulting in a highly efficient finite element simulation. The finite element mesh has 166,090 elements. Since the velocity degrees of freedom corresponding to the nodes for the bubble function at the centroid of the elements are eliminated by static condensation, the finite element mesh has only 35,375 nodes at element vertices. The geometric parameters for the flat die in Fig. 2, which are taken from reference [6], are given in Table 1. The die has a relatively

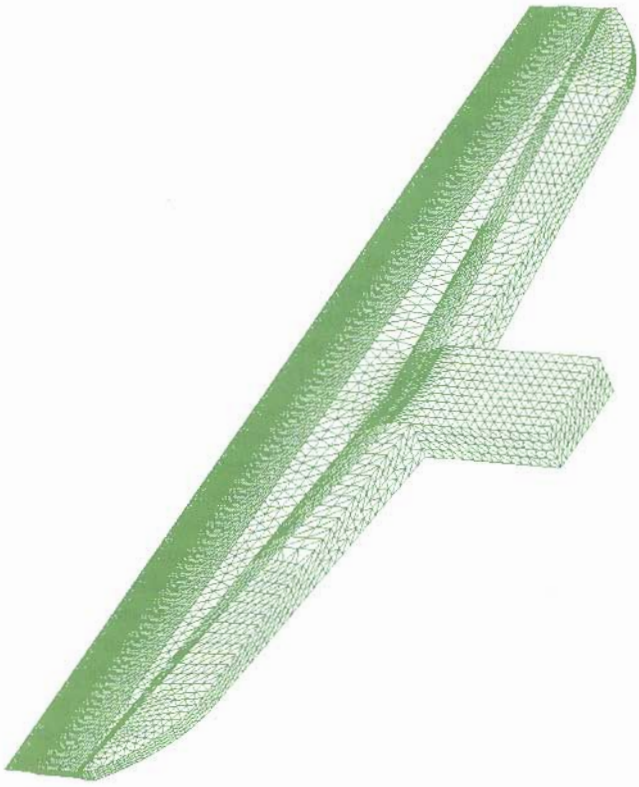

Fig. 2. Finite element mesh in the flat die

small primary manifold and a long secondary manifold before the land near the die exit. A triangular preland section is located between the primary and secondary manifolds. The extra pressure drop near the middle of the triangular preland compensates the non-uniform pressure in the primary manifold, which decreases with the distance from the feed point.

Figs. 3 and 4 compare the velocity distributions in the mid-plane of the flat die predicted by the generalized Newtonian formulation (Figs. 3A and 4A) and by the PELDOM software which includes the effect of elongational viscosity on the flow (Figs. 3B and 4B). In comparison to the velocity distributions in Figs. 3A and 4A, the distributions in Figs. 3B and 4B, respectively, have some minor differences only. Since the flow is elongational in nature near the entrance of primary manifold, the velocity distribution in this region in Fig. 3A is somewhat different from that in Fig. 3B. Before exiting the die, the polymer goes through a thin land, which has an opening of 0.102 cm in the thickness direction and is 2.54 cm long along the flow direction. Since the flow in this thin and long land before the die exit is highly shear dominated, the elongational viscosity has only a minor effect on the velocity distribution at the die exit. The velocity distribution at the exit of the flat die predicted by the PELDOM software (Fig. 3B) is slightly more uniform. Accordingly, for the same flow rate, the maximum velocity in Fig. 3B (0.304 m/s) is slightly lower than that in Fig. 3A (0.306 m/s).

The goal in design of a flat die is to obtain a uniform thickness across the width of the extruded sheet. The velocity and temperature distributions across the width of the die exit can significantly affect the thickness of the sheet. The sheet is gen-

Lengths	cm (inches)
Die width	101.6 (40)
Die length (including channel)	33.0 (13)
Inlet width	10.16 (4)
Manifold center depth	3.81 (1.5)
Manifold side depth	1.02 (0.4)
Manifold center flat length (including radius)	1.52 (0.6)
Manifold side flat length (including radius)	1.02 (0.4)
Manifold end sweep length	10.16 (4)
Preland gap	0.61 (0.24)
Preland center length	5.08 (2)
Preland side length	0.00254 (0.001)
Secondary manifold center length	5.08 (2)
Secondary manifold side length	5.08 (2)
Secondary manifold depth	0.635 (0.25)
Land length	2.54 (1)
Land gap in center	0.102 (0.04)
Angles	**Degrees**
Manifold backwall angle	85°
Manifold angle	20°
Secondary manifold angle	20°

Table 1. Geometric parameters [6] for the flat die in Fig. 2

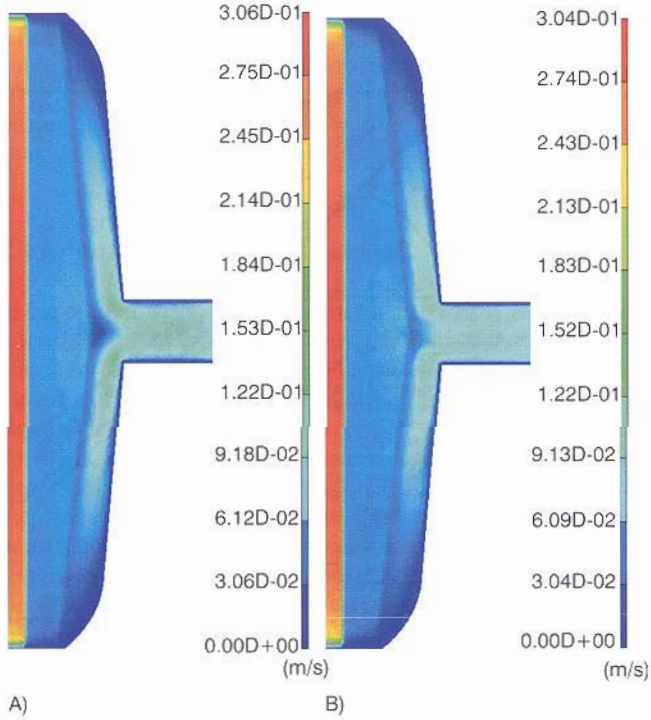

Fig. 3. Magnitude of velocity in the mid-plane of the flat die. A: Carreau model with generalized Newtonian formulation, B: Carreau model for shear viscosity along with Sarkar-Gupta model for elongational viscosity

erally thicker at the locations with higher velocity at the die exit. Accordingly, in comparison to the sheet thickness near the two ends, the LDPE sheet extruded by the flat die in Fig. 2 is expected to have a slightly larger thickness near the center. Except at the small regions near the ends, the predicted velocity in most of the die exit is quite uniform. Therefore, the die in Fig. 2 is well balanced for Dow 132i.

Since the velocity distributions in Fig. 3A and B are very similar, it may be expected that the elongational viscosity of Dow 132i has only a minor effect on the thickness of the extruded sheet. However, the temperature of the plastic at the die exit also affects the final sheet thickness. If the velocity across the die exit is uniform, because of the higher shrinkage during cooling of the sheet, thickness is expected to be smaller at the locations with higher temperature. Fig. 5 compares the temperature distributions in the mid plane of the flat die predicted by a generalized Newtonian formulation (Fig. 5A) and by including the effect of elongational viscosity using the PELDOM software (Fig. 5B). Unexpectedly, the predicted temperature across the exit of the die is not uniform. Instead, bands of high and low temperatures are observed across the width of the die. These bands, which are formed due to variation in viscous dissipations across the die, are sometimes observed in flat die experiments. However, due to lack of experimental data, formation of temperature bands could not be verified for the die analyzed in this work. The temperature distributions at the die exit in Figs. 5A and B are significantly different, with the temperature at many locations along the die exit in Fig. 5B about 8 degrees higher than that in Fig. 5A. The difference in the temperature in Figs. 5A and B can affect the final thickness of the extruded sheet. It is noted that the main difference in the temperature distributions in Figs. 5A and B is in the land near the exit of the die. Away from the exit, the temperature distributions in Figs. 5A and B have some minor differences only. Since the flow in the land near the die exit is highly shear dominated, the large difference in temperature near the exit in Figs. 5A and B is somewhat unexpected at a first glance. However, it is noted that in the die shown in Fig. 2, just before the land, there is a large reduction in the die thickness. The flow in this converging region before the land is highly elongation dominated. In the plane of symmetry parallel to the thickness direction, Fig. 6 shows the temperature distribution in this elongation-dominated region near the exit of the flat die. It is evident in Fig. 6 that the temperature of polymer in the elongation-dominated region increases significantly when the effect of elongational viscosity is included in the simulation. With the effect of elongational viscosity included in the simulation, extra work is done to push the polymer through the elongation-dominated region. This extra work is converted into heat resulting in the higher temperature in the converging region before the land. In other words, in elongation-dominated flows the heat generated due to viscous dissipation strongly depends on the elongational viscosity of the polymer. This extra heat generated due to the high elongational viscosity of the polymer, which is being captured by the flow simulation using the PELDOM software, is convected along

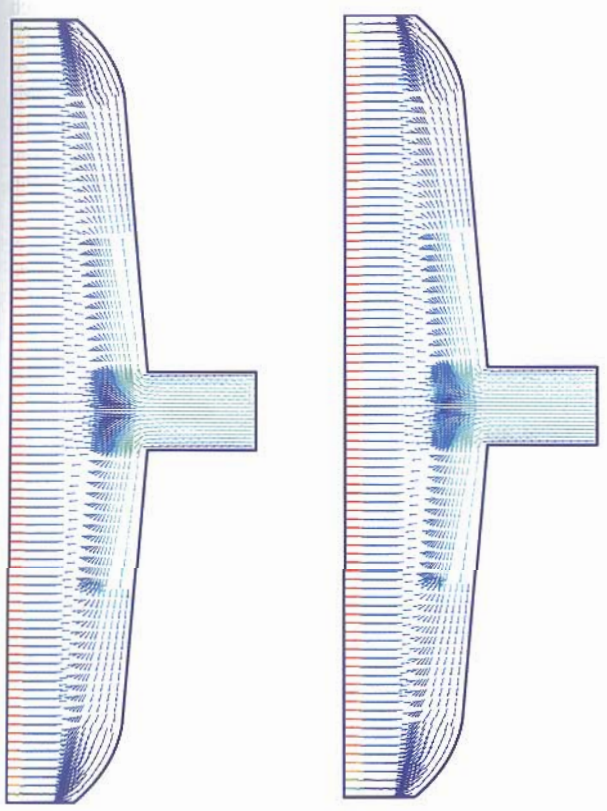

Fig. 4. Direction of velocity in the midplane of the flat die. A: Carreau model with generalized Newtonian formulation, B: Carreau model for shear viscosity along with Sarkar-Gupta model for elongational viscosity

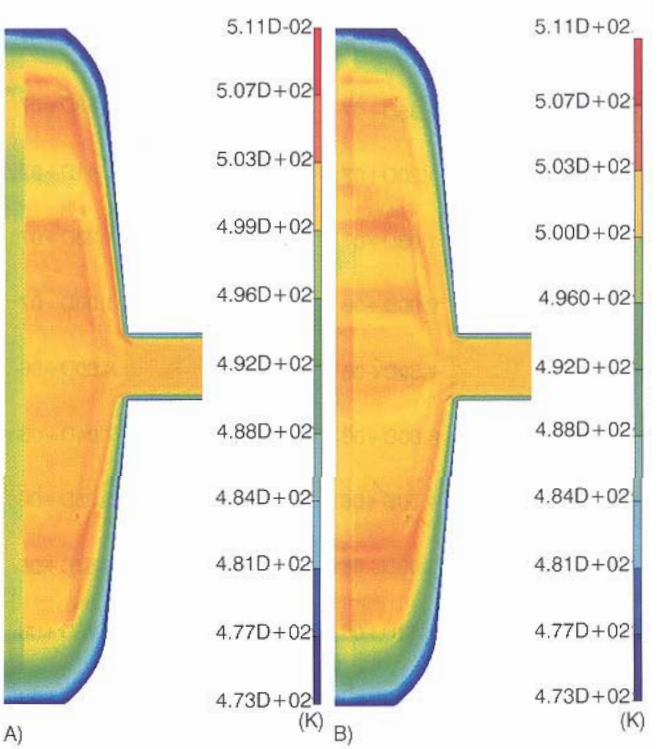

Fig. 5. Temperature distribution in the mid-plane of the flat die. A: Carreau model with generalized Newtonian formulation, B: Carreau model for shear viscosity along with Sarkar-Gupta model for elongational viscosity

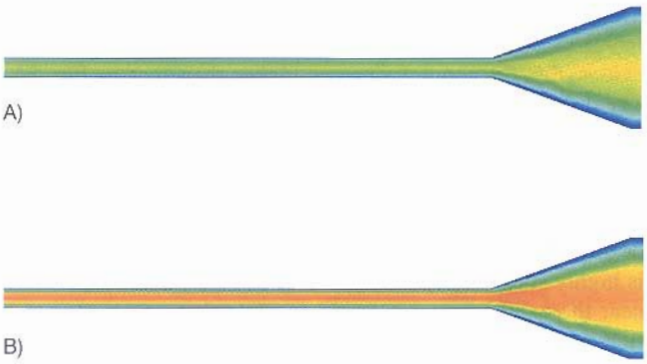

Fig. 6. Temperature distribution in the mid-plane parallel to the thickness direction of the flat die. A: Carreau model with generalized Newtonian formulation, B: Carreau model for shear viscosity along with Sarkar-Gupta model for elongational viscosity

the die land, resulting in the higher temperature at the exit in Figs. 5B and 6B.

Fig. 7 compares the pressure distributions in the mid-plane of the flat die, predicted by the generalized Newtonian formulation (Fig. 7A) and by the PELDOM software including the effect of elongational viscosity on the flow (Fig. 7B). The corresponding pressure variation along the axis of the die is shown in Fig. 8. In Figs. 7 and 8, when the effect of elongational viscosity is included in the simulation, the predicted pressure drop across the die is about 17 % larger than the pressure drop predicted by the generalized Newtonian formulation. It is evident from Fig. 8 that most of this extra pressure drop due to the high

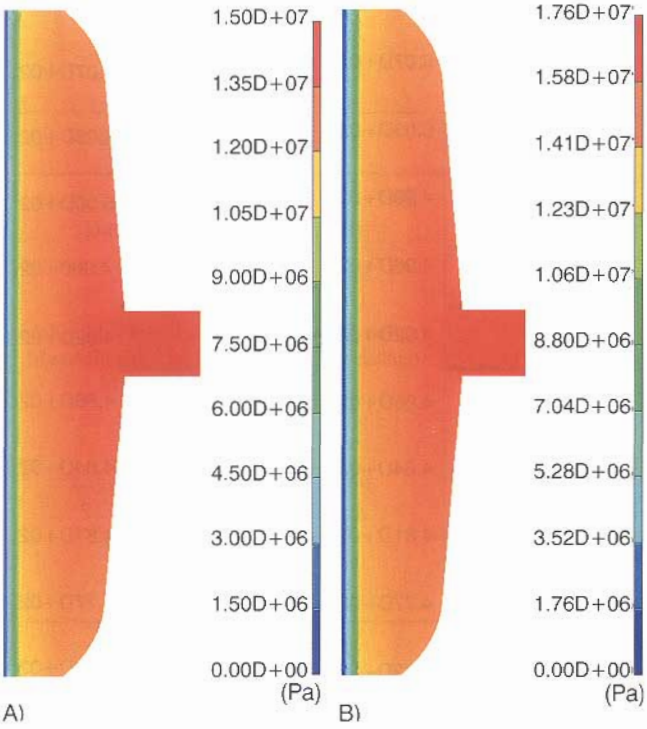

Fig. 7. Pressure distribution in the mid-plane of the flat die. A: Carreau model with generalized Newtonian formulation, B: Carreau model for shear viscosity along with Sarkar-Gupta model for elongational viscosity

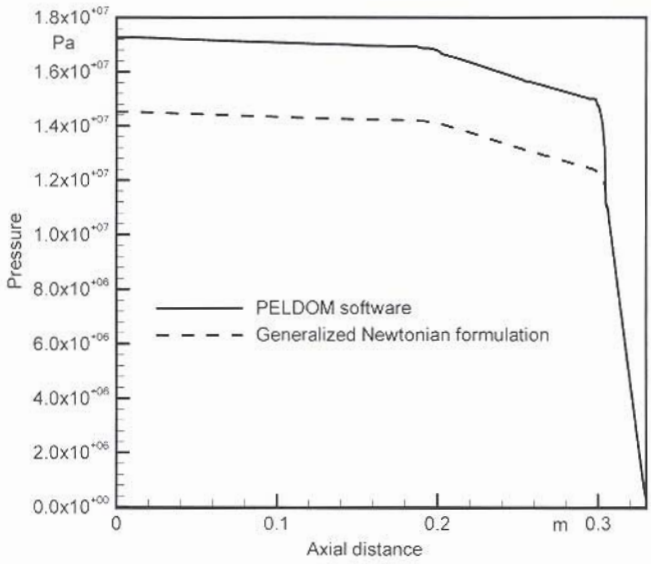

Fig. 8. Pressure variation along the axis of the flat die. The solid curve is obtained by using the Carreau model for shear viscosity along with the Sarkar-Gupta model for elongational viscosity, whereas the dashed line is obtained using the Carreau model with the generalized Newtonian formulation

elongational viscosity of the polymer is in the small converging region before the land near the exit of the die. When the effect of elongational viscosity is included in the simulation, a much larger pressure gradient is required to push the polymer through the elongation-dominated region near the entrance of the die land. Since the flow upstream and downstream of this converging region is mostly shear dominated, elongational viscosity has little effect on the pressure gradient away from the converging region. The extra pressure drop due to the high elongational viscosity of Dow 132i implies that in a screw extruder, if a constant pressure is available at the die entrance, the actual flow rate in the die will be smaller than the flow rate predicted by a flow simulation using the generalized Newtonian formulation.

4 Conclusions

The axisymmetric and planar elongational viscosities of Dow 132i, estimated by *Beaupre* and *Gupta* [15] using entrance-flow method, were used in the present work to simulate the flow in a flat die. For the flow of Dow 132i in the flat die used, the elongational viscosity is found to have only a minor effect on the velocity at the die exit. However, the predicted pressure drop in the die and the temperature distribution at the die exit changed significantly when the effect of elongational viscosity was included in the simulation.

References

1 *Tadmor, Z., Klien, I.:* Engineering Principles of Plasticating Extrusion. Van Nostrand Reinhold, New York (1970)
2 *Michaelli, W.:* Extrusion Dies for Plastics and Rubber. Hanser, Munich New York (1992)

3 *Gupta, M., Jaluria, Y., Sernas, V., Esseghir, M., Kwon, T. H.:* Poly. Eng. Sci. 33, p. 393 (1993)
4 *Shankar, R., Ramanathan, R.:* SPE ANTEC Tech. Papers 41, p. 65 (1995)
5 *Gifford, W. A.:* SPE ANTEC Tech. Papers 44, p. 290 (1998)
6 *Gifford, W. A.:* Poly. Eng. Sci. 41, p. 1886 (2001)
7 *Larson, R. G.:* Constitutive Equations for Polymeric Melts and Solutions. Butterworths, Boston (1988)
8 PELDOM software, Plastic Flow, LLC, 1206 Birch Street, Houghton, MI 49931 (www.plasticflow.com)
9 *Gupta, M.:* Poly. Eng. Sci. 40, p. 23 (2000)
10 *Sarkar, D., Gupta, M.*, in: CAE and Related Innovations for Polymer Processing. *Tsung, L.-S., Wang, H.-P., Ramani, K., Bernard, A.* (Eds.), ASME MD-Vol. 90, p. 175 (2000)
11 *Gupta, M.:* J. Reinf. Plast. Comp. 20, p. 341 (2001)
12 *Gupta, M.:* J. Reinf. Plast. Comp. 20, p. 1464 (2001)
13 *Meissner, J.:* Rheol Acta 8, p. 78 (1969)
14 *Macosko, C. W.:* Rheology Principles, Measurements and Applications, VCH: New York (1994).
15 *Beaupre, P., Gupta, M.:* SPE ANTEC Tech. Papers 48, p. 892 (2002)
16 *Sarkar, D., Gupta, M.:* J. Reinf. Plast. Comp. 20, p. 1473 (2001)
17 *Bird, R. B., Armstrong, R. C., Hassager, O.:* Dynamics of Polymeric Liquids, Vol. 1 and 2. Wiley, New York (1987)
18 *Cogswell, F. N.:* Poly. Eng. Sci. 12, p. 64 (1972)
19 *Binding, D. M.:* Non-Newt. Fluid Mech. 27, p. 193 (1988)
20 *Pichelin, E., Coupez, T.:* Comput. Mechods Appl. Mech. Eng. 163, p. 359 (1998)
21 *Bathe, K. J.:* Finite Element Procedures, Prentice Hall, New Jersey (1996).

Acknowledgements

This work was supported by the National Science Foundation Grant DMI-0200091.

Date received: July 28, 2003
Date accepted: August 28, 2003